Geotech Geol Eng (2017) 35:1783–1791
DOI 10.1007/s10706-017-0208-x

ORIGINAL PAPER

Factors Affecting Post-cyclic Undrained Shear Strength of Marine Clay

Balaji Paramasivam · Subhadeep Banerjee

Received: 5 June 2014 / Accepted: 10 March 2017 / Published online: 15 March 2017

Abstract Post-cyclic undrained shear strength is primarily controlled by the cyclic loading parameters and loading conditions. In the present paper, series of undrained constant strain cyclic triaxial test followed by strain-controlled monotonic shearing was carried out on normally consolidated marine clay specimens. An attempt was made to study the variation of post-cyclic undrained shear strength with the cyclic loading conditions namely staged cyclic loading and continuous cyclic loading. The effect of cyclic loading parameters such as cyclic strain amplitude, cyclic loading frequency and drainage after the undrained cyclic loading on post-cyclic strength and stiffness is also presented. It is observed from test results that the post-cyclic undrained strength and stiffness of the specimen is greatly influenced by the cyclic loading condition and drainage after cyclic loading. It was noted that due to the multiple stages of cyclic loading followed by pore pressure dissipation, the induced apparent overconsolidation ratio is higher for staged cyclic loading than the continuous cyclic loading conditions.

Keywords Cyclic loading · Post-cyclic strength · Recompression

B. Paramasivam (✉) · S. Banerjee
Department of Civil Engineering, Indian Institute of Technology – Madras, Chennai 600036, India
e-mail: balamani.cd@gmail.com

S. Banerjee
e-mail: subhadeep@iitm.ac.in

1 Introduction

The dynamic loading conditions such as earthquake, traffic and wave loading often induce undrained cyclic shearing on clayey soils. While many studies are carried out on the behavior of clay under cyclic loading, much of the research to date deal with specific aspects, such as low-amplitude shear modulus (Kokusho et al. 1982; Viggiani and Atkinson 1995), modulus reduction and damping ratio variation with strain (Hardin and Drnevich 1972a, b; Vucetic and Dobry 1991; Kagawa 1992; Puzrin et al. 1995), stiffness and strength degradation under cyclic loading (Vucetic and Dobry 1988; Idriss et al. 1978) as well as effective stress and pore pressure response (Zergoun and Vaid 1994; Matasovic and Vucetic 1995). It was also observed that the sample, subjected to cyclic loading followed by an undrained monotonic shearing, exhibited less undrained strength than the sample without prior cyclic loading (Thiers and Seed 1969; Taylor and Bucchus 1969; Koutsoftas 1978; Anderson et al. 1980). The possible reason, as postulated, was the reduction in effective stress by increasing cyclic pore pressure, which led to instability over soil sample. In view of this a few researchers commented that the post-cyclic stress–strain behavior were similar to the standard stress–strain behavior of OC clay (Yasuhara et al. 1992; Yasuhara 1985).

Though there are few studies reported on post-cyclic strength of clay in general, the factors controlling the post cyclic strength is not well understood. In past it was believed that the post-cyclic strength primarily depend on the maximum axial strain developed during the cyclic loading (Thiers and Seed 1969; Taylor and Bucchus 1969). However the study on Darmmen clay by Anderson et al. (1980) highlighted that apart from the maximum strain, number of cycles also influence the post-cyclic undrained strength. Jinto (1990) presented that generation on pore pressure on the soil specimen depends on the type of cyclic loading. It was noted that strain-controlled cyclic loading generates the excess pore pressure fast and it reaches equilibrium in earlier cycles than the stress-controlled cyclic loading. Additionally post-cyclic undrained shear strength may also increase or decrease depending on the drainage conditions (Yasuhara et al. 1992; Yasuhara 1985). It can therefore be summarized that the post-cyclic behaviour of soil mainly depends on the cyclic loading parameters such as cyclic strain amplitude, loading frequency and drainage after the cyclic loading.

In the present study, the marine clay specimen was subjected to constant strain undrained cyclic loading applied under two different conditions, namely staged cyclic loading (SC) and continuous cyclic loading (CC). The effect of cyclic loading conditions and loading frequency on cyclic and post-cyclic behaviour of marine clay was studied. The hysteretic energy absorbed during different type of cyclic loading was also presented. In all the tests, pore pressure generated during the cyclic test was allowed to dissipate before the post-cyclic undrained shearing.

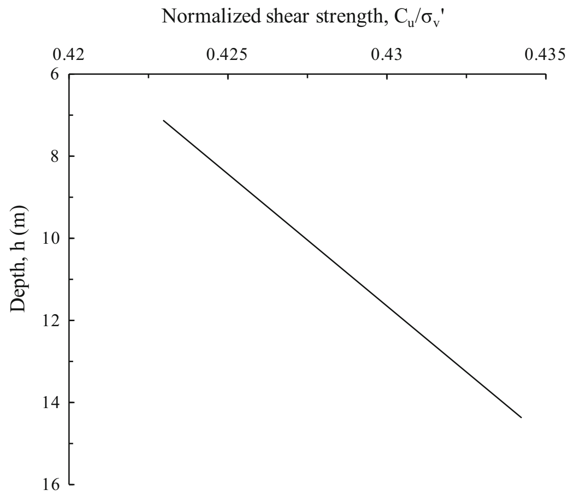

Fig. 1 Normalized undrained strength profile along depth

Table 1 Index properties of marine clay

Index properties	Values
Plasticity characteristic	
Liquid limit (%)	53
Plastic limit (%)	28
Plasticity index (%)	25
Specific gravity	2.66
Grain size distribution	
Clay size (%)	44
Silt size (%)	46
Sand (%)	10

2 Experimental Program

2.1 Soil Sample and Test Specimen Preparation

The marine clay sample used in this study was procured from coastal area of Chennai, India. Figure 1 shows the normalized strength profile along the depth. The index properties of the sample are shown in Table 1. All the experiments were carried out on reconstituted marine clay specimens prepared from slurry consolidation. The air dried clay sample, which passes through 2 mm sieve, was thoroughly mixed with water content 1.5 times of the liquid limit. The slurry was then poured into a cylindrical mould of 50 mm in diameter and 200 mm in height provided with drainage at both top and bottom ends. Figure 2 shows the schematic representation of sampling mould and loading frame. The side wall of the mould was lubricated with silicone gel. Clay slurry was then allowed to pre-consolidate under a final pressure of 80 kPa applied at equal increments. The pre-consolidated clay specimens of size 50 mm in diameter and 100 mm in height were trimmed for undrained static triaxial test (CIU) and two-way strain controlled cyclic tri-axial tests.

2.2 Experimental Procedure

The cyclic loading on specimen was carried out on pneumatic controlled cyclic tri-axial equipment. The tests were done with saturation and consolidation process followed by cyclic shearing. The saturation was done by gradual application of back pressure and by checking corresponding B-values. Back pressure is applied incrementally at the top of the specimen and is

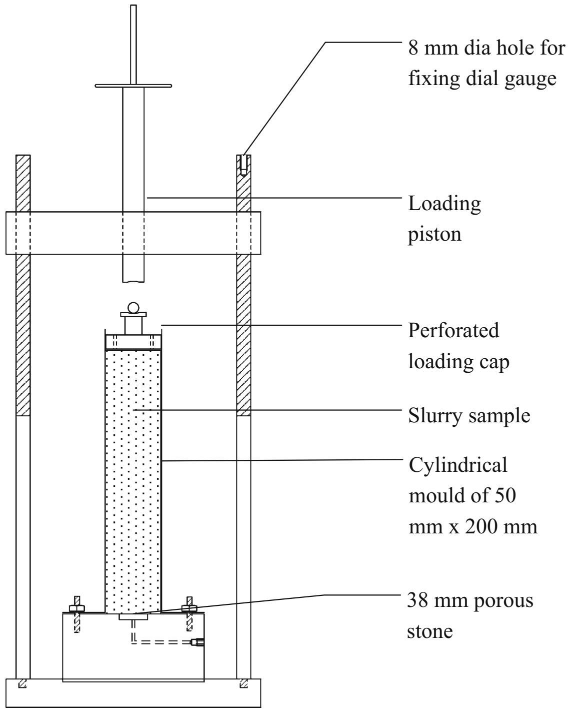

Fig. 2 Schematic diagram of mould and loading frame

undergone saturation until B-values were of the order of 0.95–0.97. After the complete saturation, marine clay specimens were subjected to effective isotropic consolidation pressure of 150 kPa. Table 2 shows the summary of the different tests conducted for the study. The three cyclic strain amplitudes were applied in two conditions, namely, staged cyclic loading (SC) and continuous cyclic loading (CC) (Teachavorasinskun et al. 2001). Figure 3 shows the schematic of the two types of the tests.

In SC tests, isotropically consolidated specimen was subjected to consecutive steps of undrained cyclic shearing from strain amplitude of 0.25% to strain amplitude of 0.7 or 1.0%. The number of loading cycles remains constant for all strain amplitude. The pore pressure generated during the cyclic load was allowed to dissipate by re-consolidating the specimen to its initial effective confining stress (150 kPa). The period of 8 h of consolidation is allowed between the stages of cyclic loading in SC tests and before the undrained post-cyclic shearing. These 8 h of consolidation period was allowed to completely dissipate the excess cyclic pore pressure. Volumetric strain also becomes constant in this period.

Table 2 Summary of test conducted in this study

Loading frequency	Type of test	Single strain amplitude
0.1 Hz	SC	0.25,0.35 and 0.7%
	SC	0.25, 0.35 and 1.0%
	CC	0.25%
	CC	0.7%
	CC	1.0%
0.5 Hz	SC	0.25, 0.35 and 0.7%
	SC	0.25, 0.35 and 1.0%
	CC	0.25%
	CC	0.7%
	CC	1.0%
1.0 Hz	SC	0.25, 0.35 and 0.7%
	SC	0.25, 0.35 and 1.0%
	CC	0.25%
	CC	0.7%
	CC	1.0%

In CC tests, separate specimens were used for all three cyclic strain amplitudes. The isotropically consolidated specimen was subjected to single cyclic strain amplitude and followed by shearing. Prior to undrained monotonic shearing, the cyclic pore pressure was allowed to dissipate by consolidating the specimens.

For both the tests, after the cyclic pore pressure dissipation, specimens were monotonically sheared at a strain rate of 0.024%/min till failure. The rate of shearing was selected in such a way that pore pressure equalization was ensured. The rate of shearing was calculated based on time taken for primary consolidation procedure given by Head (1998).

3 Results and Discussions

3.1 Cyclic Triaxial Test Results

Typical cyclic test results of CC and SC tests for a loading frequency of 0.1 Hz are shown in Figs. 4 and 5. Test results shown in this section are corresponding to confining pressure of 150 kPa. Figure 4 shows the 1st cycle hysteretic stress–strain loop of CC and SC test conducted for the cyclic strain amplitude of 0.7%. It is observed from the plot that the SC test exhibits higher undrained cyclic shear stress when compared

Fig. 3 SC and CC test procedure

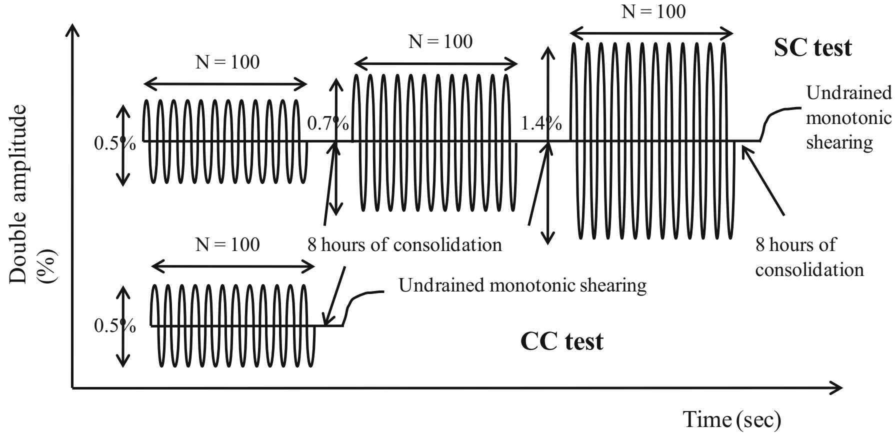

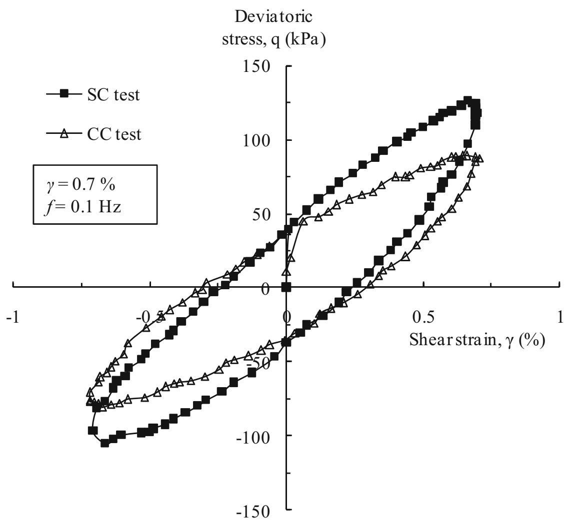

Fig. 4 Hysteretic stress strain loop of SC and CC test

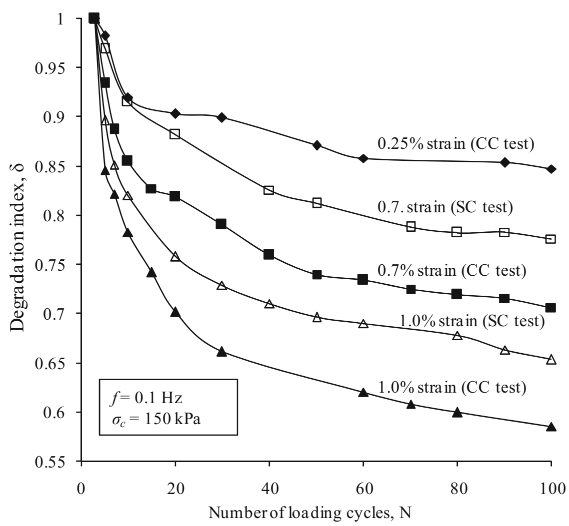

Fig. 5 Degradation index for SC and CC tests

with CC tests. This is primarily due to the effect of staged cyclic loading and followed by cyclic pore pressure dissipation at each stage which initiates apparent overconsolidation in the specimens (Aggour et al. 1987; Yasuhara et al. 1992). Undrained cyclic loading followed by dissipation of cyclic pore pressure causes reduction in void ratio. This reduction in void ratio shifts the soil condition from normal compression line to the swelling line in v-lnp' space with modified pre-consolidation pressure p_o' (Yasuhara et al. 1992). This induces the overconsolidation in the specimen and it is called apparent overconsolidation (Yasuhara 1985; Yasuhara et al. 1992). This result in higher undrained cyclic shear stress in SC tests than the CC tests.

Figure 5 shows the stiffness degradation of specimens over the loading cycles for SC and CC tests. Degradation in stiffness, during the undrained cyclic loading, is represented through the normalized parameter called degradation index δ (Idriss et al. 1978). It is defined as the ratio of the secant shear modulus at Nth cycle (G_N) to that of the first cycle secant shear modulus (G_1), as shown in Eq. 1.

$$\delta = \frac{G_N}{G_1} \tag{1}$$

Figure 5 showed that for the same cyclic strain amplitude, CC test shows higher cyclic stiffness degradation than SC test. Vucetic and Dobry (1988) reported that the degradation in stiffness reduce with the increase in overconsolidation ratio (OCR). This observation further confirms that SC tests results in apparent overconsolidation in the specimen and exhibit lesser degradation in stiffness than CC tests.

It is well known that though the damping ratio is largely frequency independent (Teachavorasinskun et al. 2001), due to the creep effect and time-dependant behavior of clayey soils, the shear modulus of the soil specimen depends on the frequency of the cyclic loading (Zavoral and Campanella 1994; Lefebvre and Leboeuf 1987). With the increase in loading rate, due to time dependent behavior, soil shows higher shear strength and lower pore pressure dissipation. The area of hysteretic stress–strain loop would also increase with the loading frequency. Figure 6 shows the variation of the dissipation of cumulative hysteretic energy during SC and CC tests along with the loading cycles conducted at constant strain amplitude of 0.7%. The cumulative hysteretic energy is the summation of the area of the hysteretic stress strain loop from the start of the test. Figure 6 shows that the energy dissipation increases with the increase in loading frequency (Lefebvre and Leboeuf 1987). It was also observed that, for all the loading frequencies, SC test shows higher energy dissipation than the CC test.

3.2 Post-cyclic Test Results

3.2.1 Effect of Loading Condition on Post-cyclic Undrained Strength

Typical test results of the post-cyclic shearing on specimens previously subjected to CC and SC tests for a frequency of 0.1 Hz are shown in Fig. 7a–c. The results of CIU test on normally consolidated specimen without prior cyclic loading are also plotted in the same figure for comparison. CIU test on marine clay specimen was carried out in Bishop-Wesley stress path apparatus. Figure 7a shows that the post-cyclic undrained shear strength is higher than the undrained strength of a sample without prior cyclic loading. Such increase in strength is attributed to the dissipation of cyclic pore pressure, prior to monotonic shearing (Yasuhara et al. 1992). Moreover, the post-cyclic undrained shear strength increases with the increase in cyclic strain amplitude. It is also noted that the axial strain to reach the peak deviatoric stress decrease with the increase in cyclic strain amplitude. This observation indicates that the specimen is apparently overconsolidated due to the prior cyclic loading, as discussed above. These observations are similar to Yasuhara (1985), Yasuhara et al. (1992) and Koutsoftas (1978).

Figure 7b plots the development of the excess pore pressure during the post-cyclic shearing. The pore pressure development during CIU test on NC clay is also potted in the same figure. Figure shows that the amount of excess pore pressure developed during post-cyclic shearing, decrease with the increase in the cyclic strain amplitude. For the same cyclic strain amplitude due to higher reduction in void ratio, SC tests report lower post-cyclic excess pore pressure than that of CC tests.

Figure 7c shows the stress path traced during the post-cyclic monotonic shearing in p'/p_e' versus q/p_e' space. The mean effective stress and deviatoric stresses are normalized with equivalent pressure p_e', which is defined as a function of specific volume (v) as shown in Eq. 2. In the Eq. 2 specific volume (v) is defined as $1 + e$, where e is the void ratio of the specimen. The parameters λ is the slope of the normally consolidated line in $v\text{-}lnp'$ space and N is the specific volume of normal compression line at $\ln p' = 1.0\ \text{kN/m}^2$. The critical state parameters N and λ are dimensionless term and it is estimated from isotropic compression test as 3.15 and 0.236, respectively.

$$p_e^{'} = \exp\left(\frac{N - v}{\lambda}\right) \tag{2}$$

Figure 7c shows that the stress path followed during the post-cyclic shearing lies left to the CIU stress path. It is well known that the CIU stress path is

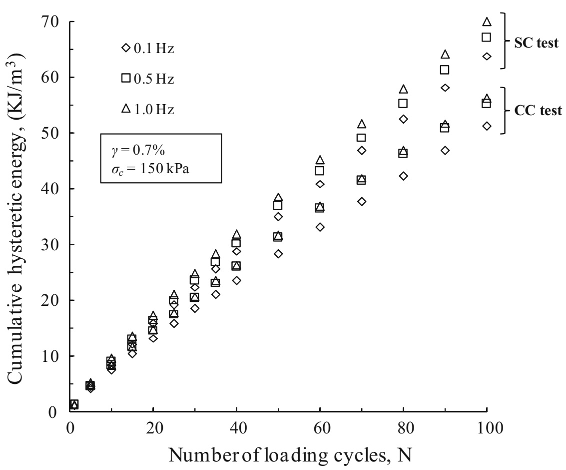

Fig. 6 Hysteretic energy dissipated versus number of loading cycle for SC and CC tests

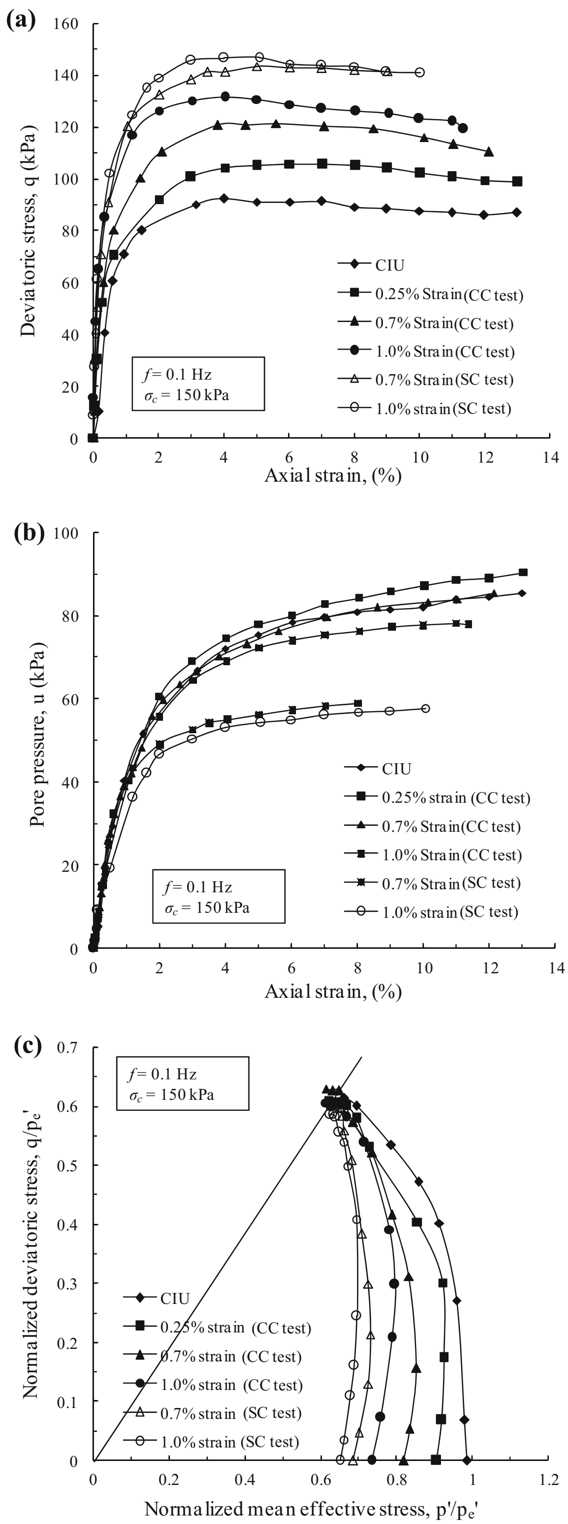

◀**Fig. 7** **a** Stress–strain response, **b** pore pressure response and **c** effective stress path of marine clay specimen during post-cyclic shearing

a virtual boundary surface beyond which no specimens would appear (Roscoe and Burland 1968). As the cyclic strain amplitude increases, stress path shifts towards left side of the state boundary surface. This indicates that the apparent overconsolidation on the specimen increases with the cyclic strain amplitude. Moreover, Fig. 7c shows that for the same cyclic strain amplitude, apparent overconsolidation on SC tests is higher than CC tests. Multi-stages of cyclic loading followed by the dissipation of pore pressure in SC tests cause more reduction in void ratio than the CC tests. Thereby, the apparent overconsolidation ratio is higher in SC test than the CC tests. As can be seen, all the tests are terminated at the critical state line indicating that the cyclic loading followed by post-cyclic monotonic shearing would not affect the critical angle of internal friction.

3.2.2 *Effect of Frequency on Post-cyclic Strength*

Figure 8 shows the normalized post-cyclic strength obtained from SC and CC tests for loading frequencies of 0.1, 0.5 and 1.0 Hz. In the Fig. 8, the post-cyclic undrained strength is normalized by the undrained strength during CIU test on NC clay. Figure 8 shows that the effect of loading frequency is predominant for SC tests where the increase in post-cyclic strength decreases with increase in loading frequency. On the other hand, in CC tests, increase in post-cyclic strength lies in a narrow region for all loading frequencies.

Figure 9 shows the total percentage reduction in void ratio for SC and CC tests, prior to post-cyclic monotonic loading, for the cyclic loading frequency of 0.1, 0.5 and 1.0 Hz. Figure plots the normalized excess pore pressure generation plotted against percentage reduction in void ratio. The final excess pore pressure developed during cyclic loading is obtained from the pore pressure transducer attached at the base pedestal of the triaxial cell. Figure 9 shows that the reduction in void ratio as well as the development of normalized cyclic pore pressure is predominant at loading

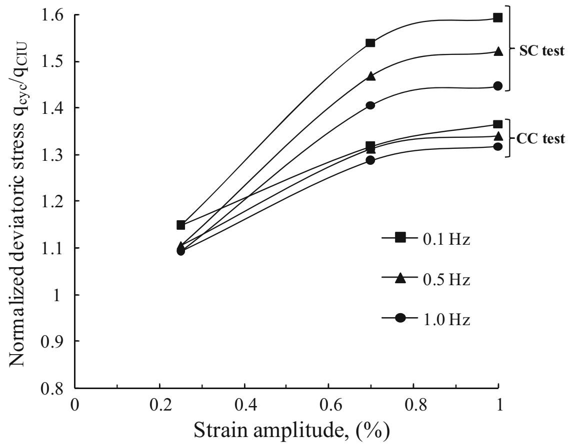

Fig. 8 Normalized post-cyclic strength for different loading frequency

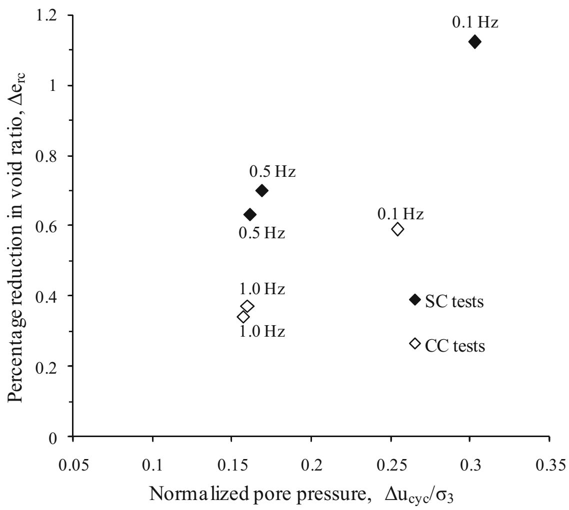

Fig. 9 Effect of loading frequency on void ratio reduction during recompression and normalized pore pressure

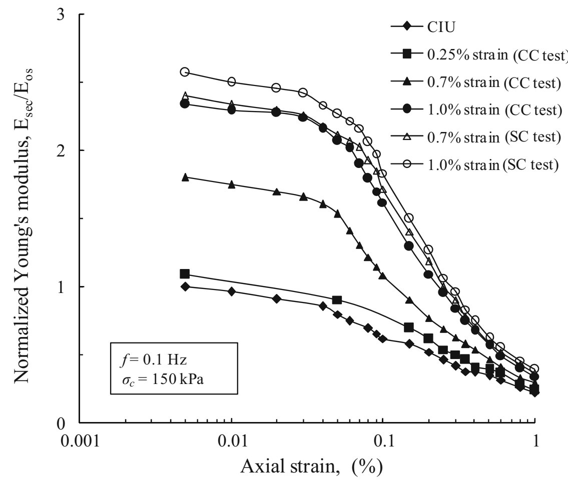

Fig. 10 Stiffness degradation of SC and CC tests

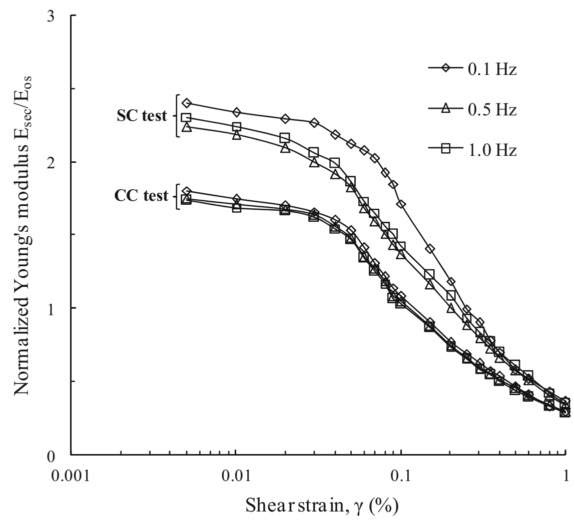

Fig. 11 Effect of loading frequency on stiffness degradation

frequency 0.1 Hz. It also indicates that, for all loading frequency, SC test undergoes considerably larger reduction in void ratio accompanied by the higher development of excess pore pressure than that of the CC tests. As a result, during post-cyclic monotonic loading, SC tests offer higher post-cyclic strength than the CC tests for all cyclic loading frequency.

3.3 Post-cyclic Stiffness Degradation

Figure 10 shows the post-cyclic modulus degradation of the SC and CC tests for the wide range of axial strain. The post-cyclic secant Young's modulus, designated as E_{sec}, is normalized with the initial secant Young's modulus (E_{os}) of specimen during static shearing. The post-cyclic secant Young's modulus of the specimen at regular interval of axial strain is estimated by calculating the slope of the straight line drawn from the origin to the respective axial strain. As can be seen from Fig. 10, the post-cyclic secant Young's modulus is higher than secant Young's modulus obtained in CIU test. This is mainly due to the dissipation of excess pore pressure developed during undrained cyclic loading, which in turn, results in reduction of void ratio and increase in stiffness of the specimen. It is also observed from Fig. 10 that the degradation of post-cyclic stiffness decreases with the increase in cyclic strain amplitude. Moreover, in comparison to CC tests, SC tests specimen undergoes relatively lower degradation in stiffness for the same cyclic strain amplitude. Such observations further corroborate the earlier results that the cyclic loading followed by drainage induce an apparent overconsolidation on the specimen and it is predominant in SC tests than the CC tests. The effect of loading frequency on stiffness degradation is shown in Fig. 11. It is observed that the loading frequency has no significant effect on the post-cyclic stiffness degradation.

4 Conclusion

The foregoing discussion suggests that the post cyclic strength is significantly influenced by several factors such as, type of cyclic loading, loading frequency, drainage condition and cyclic strain amplitudes. Some of the notable conclusions obtained from the above study are as follows:

1. Post-cyclic undrained shear strength is greatly affected by the cyclic loading condition, in addition to the cyclic loading parameters. It is observed from the test results that SC specimens tested at loading frequency of 0.1 Hz with the cyclic strain amplitude of 0.7 and 1.0% shows an increase in post-cyclic undrained shear strength of 17 and 20% than the CC tests under similar test conditions.
2. Cyclic loading followed by the dissipation of pore pressure leaves the specimen as apparently ovser-consolidated and this overconsolidation ratio is significant in SC tests than the CC tests.
3. In SC tests, post-cyclic undrained shear strength decreases with the increase in loading frequency. However, in case of CC tests, the loading frequency has negligible effect on post-cyclic undrained shear strength.
4. Due to reduction in void ratio of the specimen, prior to post-cyclic shearing, post-cyclic secant Young's modulus is higher than the Young's modulus of specimen during static shearing.
5. Post-cyclic stiffness degradation is lesser in SC tests than the CC tests, due to higher degree of overconsolidation ratio.

References

Aggour MS, Tawfiq KS, Amini F (1987) Effect of frequency content on dynamic properties for cohesive soils. In: Proceedings of 3rd international conference on earthquake engineering and soil dynamics, Princeton, vol 42, pp 31–39

Anderson KH, Pool JH, Brown SF, Rosenbrand WF (1980) Cyclic and static laboratory tests on Darmmen clay. J Geotech Eng 106(5):499–529

Hardin BO, Drnevich VP (1972a) Shear modulus and damping in soils: measurement and parameter effects. J Soil Mech Found Div 98:603–624

Hardin BO, Drnevich VP (1972b) Shear modulus and damping in soils: design equations and curves. J Soil Mech Found Div 98:667–692

Head KH (1998) Manual of soil laboratory testing, volume-3: effective stress tests. Wiley, Singapore

Idriss IM, Dobry R, Doyle EH, Singh RD (1978) Nonlinear behaviour of soft clays during cyclic loading conditions. J Geotech Geoenviron Eng 104(12):1427–1447

Jinto H (1990) Stress–strain and strength characteristics of clay during post-cyclic monotonic loading. MS Thesis, University of British Columbia, Canada

Kagawa T (1992) Moduli and damping factors of soft marine clays. J Geotech Geoenviron Eng 118(9):1360–1375

Kokusho T, Yoshida Y, Esashi Y (1982) Dynamic properties soft clay for wide strain range. Soils Found 22(4):1–18

Koutsoftas DC (1978) Effect of cyclic loads on undrained strength of two marine clays. J Geotech Geoenviron Eng 104(5):609–620

Lefebvre G, Leboeuf D (1987) Rate effects and cyclic loading of sensitive clays. J Geotech Geoenviron Eng 113(5):476–489

Matasovic N, Vucetic M (1995) Generalized cyclic-degradation-pore-pressure generation model for clays. J Geotech Geoenviron Eng 121(1):33–42

Puzrin A, Frydman S, Talesnick M (1995) Normalising degrading behaviour of soft clay under cyclic simple shear loading. J Geotech Geoenviron Eng 121(12):836–843

Roscoe KH, Burland JB (1968) On the generalized stress–strain behaviour of wet clay. In: Heyman J, Leckie FA (eds) Engineering plasticity. Cambridge University Press, Cambridge, pp 535–609

Taylor PW and Bucchus DA (1969) Dynamic cyclic strain test on a clay. In: Proceedings of 7th international Conference on soil mechanics and foundation engineering, Mexico, vol 2, pp 401–409

Teachavorasinskun S, Thongchim P, Lukkunaprajit P (2001) Shear modulus and damping ratio of a clay during undrained cyclic loading. Geotechnique 51(5):467–470

Thiers GR, Seed HB (1969) Strength and stress–strain characteristic of clay subjected to seismic loading condition. Geotech Test J STP 450:3–56

Viggiani G, Atkinson JH (1995) Stiffness of fine-grained soils at very small strains. Geotechnique 45(2):249–265

Vucetic M, Dobry R (1988) Degradation of marine clays under cyclic loading. J Geotech Eng Div 114(2):133–149

Vucetic M, Dobry R (1991) Effect of soil plasticity on cyclic response. J Geotech Eng Div 117(2):89–107

Yasuhara K (1985) Undrained and drained cyclic triaxial test on a marine clay. In: Proceedings of 11th international conference on soil mechanics and foundation engineering, Paris, France, vol 2, pp 1095–1098

Yasuhara K, Hirao K, Hyde FA (1992) Effects of cyclic loading on undrained strength and compressibility of clay. Soils Found 32(1):100–116

Zavoral DZ, Campanella RG (1994) Frequency effects on damping/modulus of cohesive soil. Geotech Test J STP 1213:191–201

Zergoun M, Vaid YP (1994) Effective stress response of clay to undrained cyclic loading. Can Geotech J 31:714–727